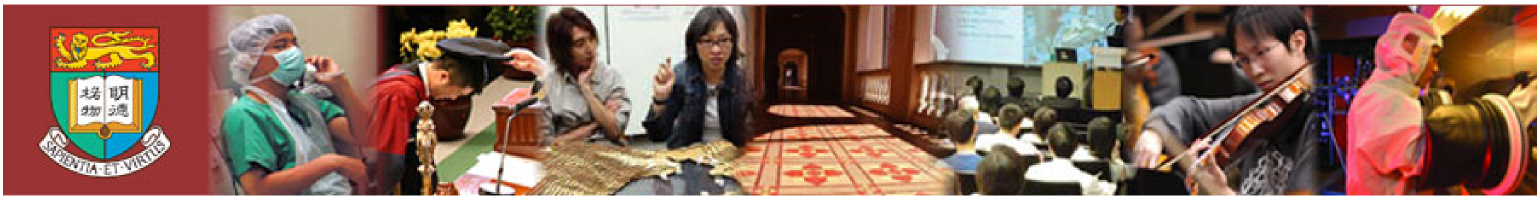

Atom-number fluctuation and macroscopic quantum entanglement in dipole spinor condensates

Yixiao Huang,[1,2,*] Zhe Sun,[3] and Xiaoguang Wang[2,†]
[1]*Department of Physics and Center of Theoretical and Computational Physics, The University of Hong Kong, Hong Kong, China*
[2]*Zhejiang Institute of Modern Physics, Department of Physics, Zhejiang University, Hangzhou 310027, China*
[3]*Department of Physics, Hangzhou Normal University, Hangzhou 310036, China*
(Received 12 January 2014; published 3 April 2014)

We study the spin distribution and macroscopic entanglement in spinor condensates confined in an anisotropic potential under external magnetic fields. Different types of magnetic phases can be reached by tuning the magnetic dipolar interaction strength by modifying the trapping geometry. We investigate the atom-number fluctuations of the ground state and show that the different internal hyperfine states exhibit super-Poissonian, Poissonian, and sub-Poissonian distributions with different trapping geometries and strengths of the external magnetic field. We also propose a scheme to create a macroscopic maximally entangled spin state by slowly sweeping the external magnetic field.

DOI: 10.1103/PhysRevA.89.043601 PACS number(s): 03.75.Gg, 03.75.Mn

I. INTRODUCTION

Bose-Einstein condensates have been studied extensively for the past ten years [1–16]. More recently, since the experimental observation of spinor condensates (condensates with spin degrees of freedom) in ^{23}Na and ^{87}Rb atoms [17–20], their magnetic properties have attracted much attention in both experimental [18] and theoretical studies [21–26]. Under a more careful inspection, the long-range magnetic dipolar interactions (which may originate from the intrinsic or induced dipole moments of the atoms or molecules [27–33]) may have a rather strong effect on the stability of the condensate [34–36] and significantly modify the excitation spectrum [37–40]. This is because even though the total s-wave collisional interaction strength is much larger than the dipolar interaction strength, the spin exchange interaction is not necessarily much stronger. A simple calculation shows that for the $f=1$ hyperfine manifold of ^{87}Rb atoms, the magnitude of the dipolar energy can be as large as 10% of the spin-exchange energy [41], thus making a nontrivial contribution to the total spin-dependent energy; moreover the long-range and anisotropic nature of the dipolar interaction may further enhance its effects.

The dipolar interaction motivated a detailed investigation of spinor condensates, and some works have explored the effect of the dipolar interactions on spinor condensates confined in multiwell potentials [42–44], where only the dipolar interactions between different potential wells are taken into account. Recently, the dipolar effects in a single trapped spinor condensate with a magnetic-field-free environment was investigated [5–11]. However, those studies mainly focus on the atoms trapped in an axially symmetric potential, $V_{\rm ext}(\mathbf{r})$, with the symmetry axis chosen to be the quantization axis. In this paper, we will consider dipolar spinor condensates confined in an anisotropic potential under external magnetic fields. Such a system can be modeled as a biaxial quantum magnet. By tuning the strength of magnetic dipole interaction, the system exhibits different magnetic structures.

In the present work, we mainly consider the atom-number fluctuation of three different internal hyperfine states in the ground state. The results show that atom-number fluctuations exhibit drastically different features in the three different phases. In region Z with easy axis along the z axis (the easy axis corresponds to the direction of minimum energy), we find the $\langle\hat{n}_0\rangle=0$ and $m_F=0$ state exhibits super-Poissonian distributions, while the $m_F=-1$ state exhibits sub-Poissonian distributions and $\langle\hat{n}_{-1}\rangle=N$. In regions X and Y (easy axis along the x and y axes, respectively), the relation between the number of different hyperfine states is given by $\langle\hat{n}_0\rangle=2\langle\hat{n}_{\pm1}\rangle\simeq N/2$. For the $m_F=0$ state, it displays sub-Poissonian distributions, while the $m_F=-1$ state exhibits three different distributions for the different strengths of the dipole interaction. We also show that the internal hyperfine states exhibit drastically different atom-number fluctuations by changing the strength of the external magnetic field. In addition, we investigate the entanglement in this system. Based on the adiabatical theorem, we propose a scheme to create a macroscopic maximally entangled spin state by slowly sweeping the external magnetic field [5,45].

This paper is organized as follows. In Sec. II, we introduce the model of spin-1 condensates with dipole interaction confined in an anisotropic potential under an external magnetic field and derive a model which corresponds to a biaxial quantum magnet. In Sec. III, we discuss the ground-state magnetic structure of the system and investigate the atom-number fluctuation in different phases. In Sec. IV, we propose a scheme to create a macroscopic maximally entangled spin state by slowly sweeping the external magnetic field. Finally, our conclusions and some remarks on our results are presented in Sec. V.

II. SPINOR CONDENSATE WITH DIPOLAR INTERACTION

We consider a dilute gas of trapped bosonic atoms with hyperfine spin $f=1$. The Hamiltonian without the dipolar interaction and under a uniform magnetic field $\mathbf{B}$, in the second

*yxhuang1226@gmail.com
†xgwang@zimp.zju.edu.cn

quantized form, reads [1,2]

$$\mathcal{H}_0 = \int d\mathbf{r}\hat{\psi}_\alpha^\dagger(\mathbf{r})\bigg[\bigg(-\frac{\hbar^2\nabla^2}{2M}+V_{\text{ext}}(\mathbf{r})\bigg)\hat{\psi}_\alpha(\mathbf{r}) - g_F\mu_B \times \mathbf{B}\cdot\mathbf{F}_{\alpha\beta}\hat{\psi}_\beta(\mathbf{r})\bigg] + \frac{c_0}{2}\int d\mathbf{r}\hat{\psi}_\alpha^\dagger(\mathbf{r})\hat{\psi}_\beta^\dagger(\mathbf{r})\hat{\psi}_\alpha(\mathbf{r})\hat{\psi}_\beta(\mathbf{r}) + \frac{c_2}{2}\int d\mathbf{r}\hat{\psi}_\alpha^\dagger(\mathbf{r})\hat{\psi}_{\alpha'}^\dagger(\mathbf{r})\mathbf{F}_{\alpha\beta}\cdot\mathbf{F}_{\alpha'\beta'}\hat{\psi}_\beta(\mathbf{r})\hat{\psi}_{\beta'}(\mathbf{r}), \tag{1}$$

where $\hat{\psi}_\alpha(\mathbf{r})$ is the atomic field annihilation operator associated with the atom in the hyperfine spin state $|f=1,m_f=\alpha\rangle(\alpha=0,\pm1)$ and $\mathbf{F}$ is the angular momentum operator. The mass of the atom is given by M, and the trapping potential $V_{\text{ext}}(\mathbf{r})$ is assumed to be spin independent. The nonlinear coefficients are given by

$$c_0 = 4\pi\hbar^2(a_0+2a_2)/(3M), \tag{2}$$

$$c_2 = 4\pi\hbar^2(a_2-a_0)/(3M), \tag{3}$$

where a_f $(f=0,2)$ is the s-wave scattering length for spin-1 atoms in the combined symmetric channel of total spin f, μ_B is the Bohr magneton, and g_F is Landé g factor.

The Hamiltonian for the dipolar interactions reads [4]

$$\mathcal{H}_{dd} = \frac{c_d}{2}\int d\mathbf{r}\int d\mathbf{r}'\frac{1}{|\mathbf{r}-\mathbf{r}'|^3} \times [\hat{\psi}_\alpha^\dagger(\mathbf{r})\hat{\psi}_{\alpha'}^\dagger(\mathbf{r}')\mathbf{F}_{\alpha\beta}\cdot\mathbf{F}_{\alpha'\beta'}\hat{\psi}_\beta(\mathbf{r})\hat{\psi}_{\beta'}(\mathbf{r}') - 3\hat{\psi}_\alpha^\dagger(\mathbf{r}) \times \hat{\psi}_{\alpha'}^\dagger(\mathbf{r}')(\mathbf{F}_{\alpha\beta}\cdot\mathbf{e})(\mathbf{F}_{\alpha'\beta'}\cdot\mathbf{e})\hat{\psi}_\beta(\mathbf{r})\hat{\psi}_{\beta'}(\mathbf{r}')], \tag{4}$$

where $\mathbf{e}=(\mathbf{r}-\mathbf{r}')/|\mathbf{r}-\mathbf{r}'|$ is a unit vector and $c_d=\mu_0 g_F^2\mu_B^2/4\pi$ is the dipolar interaction parameter, with μ_0 being the vacuum magnetic permeability. The total Hamiltonian is then $\mathcal{H}_{\text{tot}}=\mathcal{H}_0+\mathcal{H}_{dd}$. For the two experimentally realized spinor condensate systems (^{23}Na, ^{87}Rb), we have $|c_2|\ll c_0$ and $c_d\lesssim 0.1|c_2|$. Under these conditions, we can invoke the single-mode approximation (SMA) in which atoms in different spin states are described by the same wave function $\phi(\mathbf{r})$, so we can decompose the field operator as [3]

$$\hat{\psi}_\alpha(\mathbf{r}) \simeq \phi(\mathbf{r})\hat{a}_\alpha, \tag{5}$$

where $\hat{a}_\alpha$ is the annihilation operator of the spin component α.

Under SMA, the Hamiltonian without dipolar interaction reads [3]

$$\mathcal{H}_0 = c_2'\hat{\mathbf{L}}^2 - g_F\mu_B\mathbf{B}\cdot\hat{\mathbf{L}}, \tag{6}$$

where $\mathbf{B}$ is the strength of the external magnetic field. The Hamiltonian of the dipolar interaction takes the form

$$\mathcal{H}_{dd} = c_d'\big(-\hat{\mathbf{L}}^2+3\hat{L}_z^2+3\hat{a}_0^\dagger\hat{a}_0\big) + 3c_d''\big(-\hat{L}_x^2+\hat{L}_y^2+\hat{a}_{-1}^\dagger\hat{a}_1+\hat{a}_1^\dagger\hat{a}_{-1}\big), \tag{7}$$

where

$$c_d' = \frac{c_d}{4}\int d\mathbf{r}d\mathbf{r}'\frac{|\phi(\mathbf{r})|^2|\phi(\mathbf{r}')|^2}{|\mathbf{r}-\mathbf{r}'|^3}(1-3\cos^2\theta_e), \tag{8}$$

$$c_d'' = \frac{c_d}{4}\int d\mathbf{r}d\mathbf{r}'\frac{|\phi(\mathbf{r})|^2|\phi(\mathbf{r}')|^2}{|\mathbf{r}-\mathbf{r}'|^3}\sin^2\theta_e e^{\pm 2i\phi_e}, \tag{9}$$

where θ_e and ϕ_e are the polar and azimuthal angles of $(\mathbf{r}-\mathbf{r}')$, respectively. Operator $\hat{\mathbf{L}}$ in Eqs. (6) and (7) is defined as $\hat{\mathbf{L}}=\hat{a}_\alpha^\dagger\mathbf{F}_{\alpha\beta}\hat{a}_\beta$, which characterizes the total many-body angular momentum operator. It is easy to see that Hamiltonian (7) corresponds to a biaxial quantum magnet. Rescaling Hamiltonians (6) and (7) by using $|c_2'|$ as the energy unit and considering the case of $c_2<0$ for Rb atoms, which indicates that the spin-exchange interaction is ferromagnetic, the dimensionless Hamiltonian reduces to

$$\mathcal{H} = -\frac{3-D}{3}\hat{\mathbf{L}}^2 - D\hat{L}_z^2 + E\big(\hat{L}_x^2-\hat{L}_y^2\big) - \mathbf{H}\cdot\hat{\mathbf{L}} - D\hat{n}_0 - E(\hat{a}_{-1}^\dagger\hat{a}_1+\hat{a}_1^\dagger\hat{a}_{-1}), \tag{10}$$

where $D=-3c_d'/|c_2'|$, $E=-3c_d''/|c_2'|$, and $\mathbf{H}=g_F\mu_B\mathbf{B}/|c_2'|$. To get some idea of the interaction parameters, we then choose the Gaussian wave packet for the condensate wave function

$$n(\mathbf{r}) = \pi^{-3/2}(q_xq_yq_z)^{-1}e^{-x^2/q_x^2-y^2/q_y^2-z^2/q_z^2}, \tag{11}$$

which yields

$$D(\kappa_x,\kappa_y) = -\frac{4\pi c_d}{|c_2|}\kappa_x\kappa_y\int_0^\infty dt\, te^{-(\kappa_x^2+\kappa_y^2)t^2/2} \times I_0\big[\big(\kappa_x^2-\kappa_y^2\big)t^2/2\big]\big\{2-3\sqrt{\pi}te^{t^2}[1-\text{erf}(t)]\big\}, \tag{12}$$

$$E(\kappa_x,\kappa_y) = -\frac{4\pi^{3/2}c_d}{|c_2|}\kappa_x\kappa_y\int_0^\infty dt\, e^{-(\kappa_x^2+\kappa_y^2)t^2/2}t^2 \times I_1\big[\big(\kappa_x^2-\kappa_y^2\big)t^2/2\big]e^{t^2}[1-\text{erf}(t)], \tag{13}$$

with $\kappa_{x,y}\equiv q_{x,y}/q_z$, $I_0[x]$ and $I_1[x]$ being the modified Bessel functions of the first kind, and erf being the error function. Here we notice that when $E=0$, Hamiltonian (10) reduces to the uniaxial magnet [4,5].

III. SPIN STRUCTURE IN THE GROUND STATE

Equation (10) is reminiscent of the Hamiltonian describing an anisotropic quantum magnet. The ground state of the system can be found by numerically diagonalizing Hamiltonian (10). As shown in Fig. 1, the κ_x and κ_y parameter plane is divided into regions X, Y, and Z based on the ground-state wave function in the absence of magnetic field [45]. Regions X, Y, and Z represent the ferromagnetic phase with the ground states $|G\rangle=|N,\pm N\rangle_x$, $|N,\pm N\rangle_y$, and $|N,\pm N\rangle_z$ respectively, where we have introduced the standard angular momentum basis states $|l,m\rangle_{x,y,z}$ that are common eigenstates of L^2 and $L_{x,y,z}$. In the parameter region $-1\leqslant\log_{10}\kappa_{x,y}\leqslant 1$ under an arbitrary magnetic field, we find that the value of the total angular momentum is given by $\langle\hat{\mathbf{L}}^2\rangle\simeq N(N+1)$ for $N\geqslant 5$, which indicates the condensate always remains in the ferromagnetic phase with a sufficiently large number of atoms and total spin $l\simeq N$ [45]. In addition we also find that the contribution of the linear terms $[-D\hat{n}_0-E(\hat{a}_{-1}^\dagger\hat{a}_1+\hat{a}_1^\dagger\hat{a}_{-1})]$ in Hamiltonian (10) is small enough to be neglected.

First, we consider the case that a field is applied longitudinally along the positive z axis, i.e., $\mathbf{H}=H_z\hat{\mathbf{z}}$. After dropping the unimportant linear terms and the constant terms,

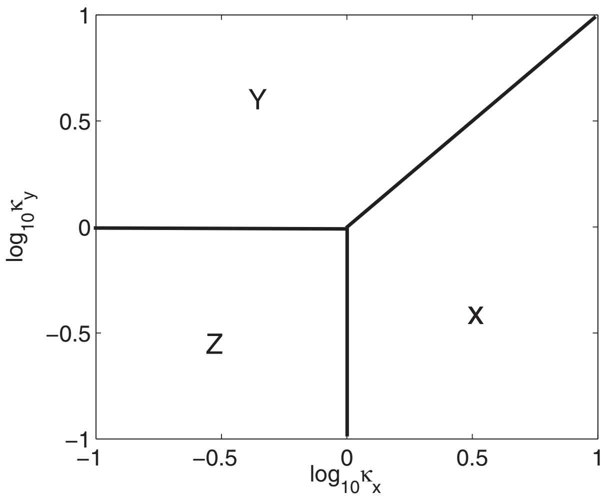

FIG. 1. Magnetic phases of a dipolar spin-1 condensate with ferromagnetic spin exchange coupling on the parameter (κ_x,κ_y) plane in the absence of external magnetic field. Regions X, Y, and Z correspond to the easy axis being along the x, y, and z axes, respectively.

the classical version of the Hamiltonian is

$$\varepsilon(\theta,\phi) = -DN^2\cos^2\theta + EN^2\sin^2\theta\cos 2\phi - H_z N\cos\theta, \tag{14}$$

where (θ,ϕ) denotes the direction of $\mathbf{L}$. The ground state (θ_0,ϕ_0) is obtained by minimizing the energy. In region Z, the ground state is given by $\theta_0 = 0$. In region Y, for $H_z < 2(E-D)N$, $\varepsilon(\theta,\phi)$ has two degenerate minima at

$$\theta_0^{(\pm)} = \pi/2 \pm \left(\pi/2 - \cos^{-1}\frac{H_z}{2(E-D)N}\right), \quad \phi_0 = \frac{\pi}{2}. \tag{15}$$

When $H_z > 2(E-D)N$, the degeneracy is removed, and the system is completely polarized by the external magnetic field. In region X, for $H_z < 2|E+D|N$, the ground state is given by

$$\theta_0^{(\pm)} = \pi/2 \pm \left(\pi/2 - \cos^{-1}\frac{H_z}{2(E+D)N}\right), \quad \phi_0 = 0. \tag{16}$$

When $H_z > 2|E+D|N$, the spin direction of the ground state is polarized along the z axis.

Now we investigate the number of atoms for different internal hyperfine states under the external magnetic field. For simplicity, here we consider a weak magnetic field. As shown in Fig. 2, in region Z (i.e., $-1 \leqslant \log_{10}\kappa_{x,y} \leqslant 0$), the atomic number of the $m_F = 0$ component is given by $\langle\hat{n}_0\rangle = 0$, and that of the $m_F = -1$ component is $\langle\hat{n}_{-1}\rangle = N$, which corresponds to the ground state $|G\rangle = |N,N\rangle_z$. In the X and Y regions, we can find $\langle\hat{n}_0\rangle \simeq N/2$ and $\langle\hat{n}_{-1}\rangle = \langle\hat{n}_1\rangle \simeq N/4$.

Next, we consider the atom-number fluctuation in terms of the Mandel Q_α parameter

$$Q_\alpha = \frac{\langle\hat{n}_\alpha^2\rangle - \langle\hat{n}_\alpha\rangle^2}{\langle\hat{n}_\alpha\rangle} - 1, \tag{17}$$

with $Q_\alpha < 0$, $Q_\alpha = 0$, and $Q_\alpha > 0$ specifying sub-Poissonian, Poissonian, and super-Poissonian distributions, respectively.

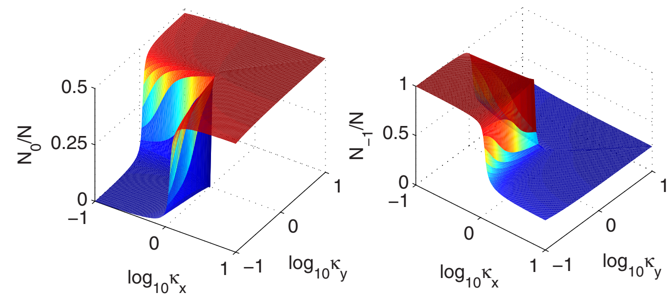

FIG. 2. (Color online) The dependence of the particle number in the hyperfine states $m_F = 0$ and -1 on the trapping geometry (κ_x,κ_y). The parameters we used here are $N = 30$, $H_z = 1$, and $c_d/|c_2| = 0.1$.

In particular, when $Q_\alpha = -1$, no atom-number fluctuations exist. In Eq. (17), $\alpha = 0, \pm 1$ correspond to three different components. As shown in Fig. 3, the numerical result shows that in regions X and Y, $Q_0 < 0$, and the $m_F = 0$ state has a sub-Poissonian distribution. However, in region Z, $Q_0 > 0$, which means that in this region the $m_F = 0$ state has a super-Poissonian distribution. At the boundaries between the different regions (Z and X, Y), Q_0 attains maximum values, which indicates the system exhibits the maximum atom-number fluctuation at the boundaries between different phases. The $m_F = -1$ state displays a sub-Poissonian distribution in region Z. At the boundaries between regions Z and X, Y, Q_{-1} attains maximum values. In regions X and Y, Q_{-1} displays different Poissonians for different κ_y and κ_y. In region X, for a fixed value of κ_y, Q_{-1} exhibits a transition from super-Poissonian to sub-Poissonian distribution as κ_x increases. However, in region Y, the spin distribution of Q_{-1} transfers from super-Poissonian to sub-Poissonian for a fixed value of κ_x as κ_y increases.

Now we consider the effect of the external magnetic field on the atom-number fluctuations. For simplicity, here we focus on region X in which the easy axis is along the x axis. First, we define the parameter

$$H_z^0 = 2|E+D|N - H_z. \tag{18}$$

With the help of Eq. (16), we can see that when $H_z^0 > 0$, two degenerate ground states exist; if $H_z^0 < 0$, the system is fully polarized along the z axis. In Fig. 4, we plot H_z^0 as a function of external magnetic field and $\log_{10}\kappa_y$ with $\log_{10}\kappa_x = 1$. We

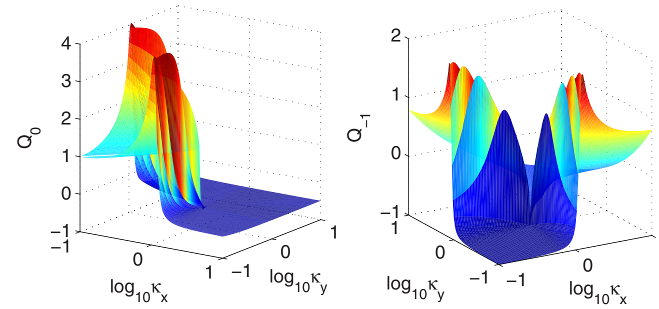

FIG. 3. (Color online) The ground-state Q parameters for the hyperfine states $m_F = 0$ and $m_F = -1$. The parameters are chosen as $N = 30$, $H_z = 1$, and $c_d/|c_2| = 0.1$.

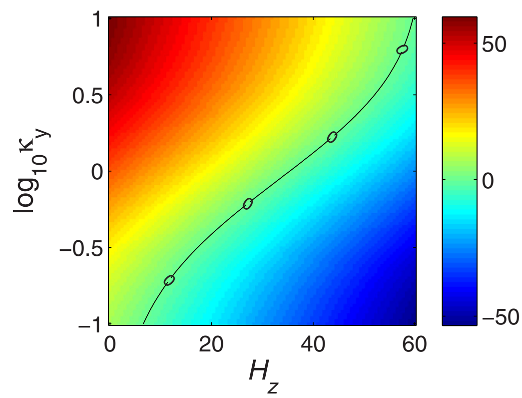

FIG. 4. (Color online) The parameter H_z^0 as a function of $\log_{10}\kappa_y$ and external magnetic field H_z with $N = 30$ and $\log_{10}\kappa_x = 1$.

can see that for a fixed value of $\log_{10}\kappa_y$, the parameter H_z^0 can be divided into two regions with H_z increasing, i.e., $H_z^0 > 0$ and <0. Next, we discuss the atom-number fluctuation. As shown in Fig. 5, the parameters $Q_{0,-1}$ are plotted as a function of H_z and $\log_{10}\kappa_y$ with $\log_{10}\kappa_x = 1$. It can be clearly seen that for a fixed value of $\log_{10}\kappa_y$, when $H_z^0 < 0$, we find $Q_0 > 0$, which means the $m_F = 0$ state exhibits a super-Poissonian distribution. When $H_z^0 > 0$, we see the $m_F = 0$ state displays a sub-Poissonian distribution. For the $m_F = -1$ state, it can been found that the value of Q_{-1} decreases as H_z increases. When $H_z > 2|E + D|N$, $Q_{-1} = -1$, which indicates that there is no atom-number fluctuation.

IV. SPIN ENTANGLEMENT

Finally, we consider the dynamic creation of maximally entangled spin states by using the condensate in region Z. Quantum entanglement has been used to perform many useful works in quantum computation and quantum information science. In the past few years, many methods have been found to create an entangled state for various physical systems, such as ion traps, nonlinear optics, nuclear magnetic resonance, and cavity quantum electrodynamics [46]. Here we adopt a scheme similar to that used in the uniaxial magnet system by sweeping the magnetic field which is vertical to the easy axis [5,45].

Before discussing the process of the scheme, we first investigate the ground state of the system under an external magnetic field along the hard axis. Without loss of generality, we focus on the region with $D > |E|$, which corresponds to the geometric parameters (κ_x, κ_y) in region Z in Fig. 1. We

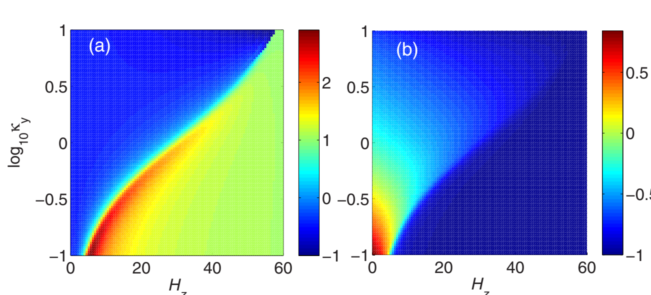

FIG. 5. (Color online) The Mandel parameters (a) Q_0 and (b) Q_{-1} as a function of H_z and $\log_{10}\kappa_y$, with $N = 30$ and $\log_{10}\kappa_x = 1$.

first apply a magnetic field along the x axis, i.e., $\mathbf{H} = H_x\hat{\mathbf{x}}$. Since we focus on the case of the ferromagnetic, we treat the total spin $\hat{\mathbf{L}}$ as a classical magnetization vector with length $|\mathbf{L}| = N$. After neglecting the unimportant linear terms and the constant terms, the energy of the system becomes

$$\varepsilon(\theta,\phi) = -DN^2\cos^2\theta + EN^2\sin^2\theta\cos 2\phi - H_xN\sin\theta\cos\phi, \qquad (19)$$

where (θ,ϕ) denotes the direction of $\mathbf{L}$. Apparently, when $H_x < H_x^* = 2N(D + E)$, the ground state is doubly degenerate, and they are located at

$$\theta_0^{(\pm)} = \frac{\pi}{2} \pm \left(\frac{\pi}{2} - \sin^{-1}\frac{H_x}{2N(D+E)}\right), \quad \phi_0 = 0. \qquad (20)$$

When $H_x > H_x^*$, the two degenerate states collapse into one, the system is fully polarized by the external field, and the two minima merge along the x axis.

Now we discuss the details of the scheme to create maximally entangled spin states. First, we introduce a time-dependent magnetic field $H_x(t)$ which is swept linearly at a constant rate $v < 0$; that is,

$$H_x(t) = H_x^{(i)} + vt \qquad (21)$$

for $t \geqslant 0$, and $H_x^{(i)} > 0$ is the initial field. Initially, we prepare the initial magnetic field to be sufficiently large, $H_x^{(i)} > H_x^*$, which means the initial state roughly stays at the $L_x = N$ level. The corresponding energy has a single minimum at $\theta = \pi/2$, $\phi = 0$. Then we slowly reduce the strength of the magnetic field; when $H_x < H_x^*$, the ground state is doubly degenerate, which corresponds to the states in Eq. (20). Then the ground state of the system becomes the symmetric quantum superposition of the two corresponding minimal-energy states. If the external field further reduces and equals zero, the minimal-energy states are given by $\theta_0 = 0$ and π, which corresponds to the quantum state $|N,\pm N\rangle_z$, and the state of the system is the maximally spin entangled Greenberger-Horne-Zeilinger (GHZ) state,

$$|\mathrm{GHZ}\rangle_z = \frac{1}{\sqrt{2}}(|N,N\rangle_z + |N,-N\rangle_z). \qquad (22)$$

In Fig. 6, the overlap between the maximally spin entangled GHZ state and the generated state is plotted as a function of the time-dependent magnetic field H_x. Figure 6 clearly shows that when the strength of the field reduces to zero, the overlap $|\langle\Psi(t)|\mathrm{GHZ}\rangle_z|^2 = 1$, which means the system generates a maximally spin entangled GHZ state.

For the scheme discussed above, we can see that the dynamical process does not rely on precise knowledge of system parameters, such as the dipole interaction strength, particle numbers, and the evolution time. As shown in Fig. 6, we just set the total particle number $N = 10$. We can also notice that over the whole process, the system is always in the minimal-energy state, which makes the system immune to the spontaneous emission-induced decoherence suffered by the electronically excited states [5]. Moreover, this scheme is rather robust; if the adiabaticity is not strictly obeyed during the evolution process, the generated state may have slightly different weights on $|N,N\rangle_z$ and $|N,-N\rangle_z$, but it remains a significantly entangled state. Also we notice that if the

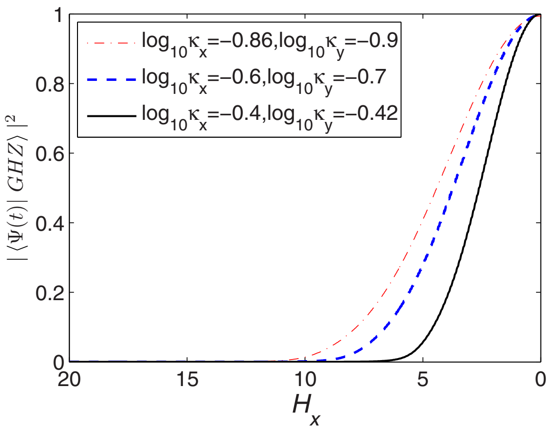

FIG. 6. (Color online) The overlap between the generated condensate state and the maximally entangled state |GHZ⟩ as a function of the magnetic-field sweep. The total number is $N = 10$, and the linear field sweeping rate $dH_x/dt = -0.08$.

magnetic field **H** is misaligned such that it forms an angle $\delta\phi$ to the z axis, it will degrade the entanglement. Finally, the evolution time can be adjusted by accelerating the sweeping rate beyond the region near the point $H_x = H_x^*$. In addition, we note that this scheme may be also applied to other biaxial magnetic materials to create an entangled state.

V. CONCLUSION

To conclude, we have studied a spinor condensate with dipole interaction confined in an anisotropic potential under external magnetic fields. Using the single-mode approximation, we show the system can be modified as a model which corresponds to a biaxial quantum magnet. Different magnetic structures can be reached by tuning the dipole interaction strength by modifying the trapping geometry. We have studied the atom-number fluctuation for the three internal hyperfine states and found that in region Z, the $m_F = 0$ state has a super-Poissonian distribution, while the $m_F = -1$ state just displays a sub-Poissonian distribution. In regions X and Y, $\langle\hat{n}_0\rangle \simeq 2\langle\hat{n}_{\pm1}\rangle \simeq N/2$, and the $m_F = 0$ state displays sub-Poissonian fluctuation, while the $m_F = -1$ state exhibits three different distributions for the different κ_x and κ_y. We also show that by increasing the strength of the external magnetic field, the internal hyperfine states exhibit drastically different quantum fluctuations.

Finally, we discuss the entanglement state generated in this system. We propose a scheme to create a macroscopic maximally entangled spin state by slowly sweeping the external magnetic field. We note that this scheme can also be applied to other biaxial magnetic materials to create an entangled state.

ACKNOWLEDGMENTS

The authors thank Zheng-Yuan Xue for valuable discussions. X.W. acknowledges support from the NFRPC through Grant No. 2012CB921602 and the NSFC through Grants No. 11025527 and No. 10935010. Z.S. acknowledges support from the National Natural Science Foundation of China under Grants No. 11005027 and No. 11375003, the Program for HNUEYT under Grant No. 2011-01-011, and the Zhejiang Natural Science Foundation with Grant No. LZ13A040002.

[1] T.-L. Ho, Phys. Rev. Lett. **81**, 742 (1998).
[2] T. Ohmi and K. Machida, J. Phys. Soc. Jpn. **67**, 1822 (1998).
[3] C. K. Law, H. Pu, and N. P. Bigelow, Phys. Rev. Lett. **81**, 5257 (1998).
[4] S. Yi and H. Pu, Phys. Rev. Lett. **97**, 020401 (2006).
[5] S. Yi and H. Pu, Phys. Rev. A **73**, 023602 (2006).
[6] D. S. Hall, M. R. Matthews, J. R. Ensher, C. E. Wieman, and E. A. Cornell, Phys. Rev. Lett. **81**, 1539 (1998).
[7] H. Pu and N. P. Bigelow, Phys. Rev. Lett. **80**, 1130 (1998); **80**, 1134 (1998).
[8] L. Yang and Y. Zhang, Phys. Rev. A **74**, 043604 (2006).
[9] R. M. Wilson, S. Ronen, and J. L. Bohn, Phys. Rev. A **80**, 023614 (2009).
[10] B. Xiong, J. Gong, H. Pu, W. Bao, and B. Li, Phys. Rev. A **79**, 013626 (2009).
[11] L. Santos and T. Pfau, Phys. Rev. Lett. **96**, 190404 (2006).
[12] A. Griesmaier, J. Werner, S. Hensler, J. Stuhler, and T. Pfau, Phys. Rev. Lett. **94**, 160401 (2005).
[13] Y. Kawaguchi, H. Saito, and M. Ueda, Phys. Rev. Lett. **96**, 080405 (2006).
[14] S. Yi, O. E. Mustecaplioğlu, C. P. Sun, and L. You, Phys. Rev. A **66**, 011601 (2002).
[15] Ying Wu, Phys. Rev. A **54**, 4534 (1996).
[16] E. V. Goldstein and P. Meystre, Phys. Rev. A **59**, 3896 (1999).
[17] D. M. Stamper-Kurn, M. R. Andrews, A. P. Chikkatur, S. Inouye, H.-J. Miesner, J. Stenger, and W. Ketterle, Phys. Rev. Lett. **80**, 2027 (1998).
[18] J. Stenger, S. Inouye, D. M. Stamper-Kurn, H.-J. Miesner, A. P. Chikkatur, and W. Ketterle, Nature (London) **396**, 345 (1998).
[19] M. Vengalattore, S. R. Leslie, J. Guzman, and D. M. Stamper-Kurn, Phys. Rev. Lett. **100**, 170403 (2008).
[20] M. D. Barrett, J. A. Sauer, and M. S. Chapman, Phys. Rev. Lett. **87**, 010404 (2001).
[21] B. D. Esry, C. H. Greene, J. P. Burke, Jr., and J. L. Bohn, Phys. Rev. Lett. **78**, 3594 (1997).
[22] C. J. Myatt, E. A. Burt, R. W. Ghrist, E. A. Cornell, and C. E. Wieman, Phys. Rev. Lett. **78**, 586 (1997).
[23] H. Pu, S. Raghavan, and N. P. Bigelow, Phys. Rev. A **61**, 023602 (2000).
[24] T.-L. Ho and S. K. Yip, Phys. Rev. Lett. **84**, 4031 (2000).
[25] M. Koashi and M. Ueda, Phys. Rev. Lett. **84**, 1066 (2000).
[26] Q. Gu, Phys. Rev. A **68**, 025601 (2003).
[27] B. Damski, L. Santos, E. Tiemann, M. Lewenstein, S. Kotochigova, P. Julienne, and P. Zoller, Phys. Rev. Lett. **90**, 110401 (2003).
[28] M. G. Moore and H. R. Sadeghpour, Phys. Rev. A **67**, 041603 (2003).

[29] H. L. Bethlem, G. Berden, F. M. H. Crompvoets, R. T. Jongma, A. J. A. van Roij, and G. Meijer, Nature (London) **406**, 491 (2000).

[30] C. H. Raymond Ooi, Phys. Rev. A **68**, 013410 (2003).

[31] J. D. Weinstein, R. deCarvalho, T. Guillet, B. Friedrich, and J. M. Doyle, Nature (London) **395**, 148 (1998).

[32] J. Kim, B. Friedrich, D. P. Katz, D. Patterson, J. D. Weinstein, R. DeCarvalho, and J. M. Doyle, Phys. Rev. Lett. **78**, 3665 (1997).

[33] S. Yi and L. You, Phys. Rev. A **61**, 041604(R) (2000); **63**, 053607 (2001).

[34] L. Santos, G. V. Shlyapnikov, P. Zoller, and M. Lewenstein, Phys. Rev. Lett. **85**, 1791 (2000).

[35] K. Goral, K. Rzazewski, and T. Pfau, Phys. Rev. A **61**, 051601(R) (2000).

[36] S. Giovanazzi, D. H. J. O'Dell, and G. Kurizki, Phys. Rev. A **63**, 031603(R) (2001).

[37] L. Santos, G. V. Shlyapnikov, and M. Lewenstein, Phys. Rev. Lett. **90**, 250403 (2003).

[38] S. Yi and L. You, Phys. Rev. A **66**, 013607 (2002).

[39] D. H. J. O'Dell, S. Giovanazzi, and G. Kurizki, Phys. Rev. Lett. **90**, 110402 (2003).

[40] K. Goral and L. Santos, Phys. Rev. A **66**, 023613 (2002).

[41] S. Yi, L. You, and H. Pu, Phys. Rev. Lett. **93**, 040403 (2004).

[42] H. Pu, W. Zhang, and P. Meystre, Phys. Rev. Lett. **87**, 140405 (2001).

[43] W. Zhang, H. Pu, C. Search, and P. Meystre, Phys. Rev. Lett. **88**, 060401 (2002).

[44] K. Gross, C. P. Search, H. Pu, W. Zhang, and P. Meystre, Phys. Rev. A **66**, 033603 (2002).

[45] Y. X. Huang, Y. B. Zhang, R. Lü, X. G. Wang, and S. Yi, Phys. Rev. A **86**, 043625 (2012).

[46] M. A. Nielsen and I. L. Chuang, *Quantum Computation and Quantum Communication* (Cambridge University Press, Cambridge, 2000).